THE LAMINAR-TURBULENT TRANSITION OF YIELD STRESS FLUIDS IN LARGE PIPES

S. Mitchell* and T. Myers†

Problem presented by: Prof. P. Slatter,[1]
Problem participants: M. Lombe, V. Masanja, S. Moyo, G. Muchatibaya, E. Mureithi, M. Ntunka and S. Tshehla.

Abstract

The work in this paper concerns the axisymmetric pipe flow of a Herschel-Bulkley fluid, with the aim of determining a relation between the critical velocity (defining the transition between laminar and turbulent flow) and the pipe diameter in terms of the Reynolds number Re_3. The asymptotic behaviour for large and small pipes is examined and simple expressions for the leading order terms are presented. Results are then compared with experimental data. A nonlinear regression analysis shows that for the tested fluids the transition occurs at similar values to the Newtonian case, namely in the range $2100 < \mathrm{Re}_3 < 2500$.

1 Introduction

Yield stress fluids are transported through pipes in a number of different industries, such as the transport of crude oil, mining slurries, liquid food, bio-fluids

*Department of Mathematics and Applied Mathematics, University of Cape Town, Rondebosch 7701, South Africa. *e-mail: sarah@maths.uct.ac.za*

†Department of Mathematics and Applied Mathematics, University of Cape Town, Rondebosch 7701, South Africa. *e-mail: myers@maths.uct.ac.za*

[1]Flow Process Research Centre, School of Civil Engineering, Cape Peninsula University of Technology, Bellville 7535, South Africa.

or sewage sludge, see [5, 7, 9] for example. To prevent blockage of the pipe, any coarse settleable material present must be kept suspended. This is achieved by keeping the velocity sufficiently high so that the flow remains turbulent. However, the higher the velocity, the more expensive the operation and consequently designers and operators attempt to maintain the flow at a level only slightly above the laminar-turbulent transition point. Obviously this is a risky strategy, errors can lead to expensive pipe blockage, and so it is critical that this transition point is accurately identified.

The laminar-turbulent transition point for Newtonian fluids is well known and defined in terms of the Reynolds number,

$$Re = \frac{\rho V D}{\eta} \approx 2300 \ , \tag{1}$$

where the notation is defined with the other nomenclature in Section 6. For yield stress fluids the matter is not so simple, one problem being that there is not a unique definition for the Reynolds number for these fluids. Metzner & Reed [6] proposed a generalised Reynolds number

$$Re_{MR} = \frac{8\rho V^2}{\tau_{0_l}} \ , \tag{2}$$

where τ_{0_l} should be evaluated for laminar flow conditions. Wasp *et al* [16] define a Reynolds number based on the Hedstrom number

$$Re_W = 1500\left(1 + \sqrt{1 + \frac{\rho D^2 \tau_y}{4500 K^2}}\right) \tag{3}$$

A common generalisation of the Newtonian Reynolds number, Re_w, involves defining the viscosity at the wall, so $\eta = \eta_w$, where η_w is the ratio of the shear stress and shear rate at the wall, see [2, 8, 15] for example. For a yield stress fluid flowing in a pipe, Slatter [9, 12] proposes a formulation that takes this concept even further. Instead of focussing on the flow solely at the pipe wall they include the flow in the annular region surrounding the central plug. The plug flow is neglected based on the premise that this does not form part of the sheared region, and is not behaving as a fluid. The analysis leads to what is termed Re_3 where

$$Re_3 = \frac{8\rho V_a^2}{\tau_y + K\left(\frac{8V_a}{D_a}\right)^n} \ . \tag{4}$$

Not only is the appropriate form of the Reynolds number the subject of debate, there is also confusion over the value at which the transition occurs, although this is most likely fluid dependent. In [3] the flow of a Laponite fluid (a water and synthetic clay mixture) is investigated, using a Herschel-Bulkley model, and their experiments indicate a transition to turbulence for $Re_w \sim 3400$. Rudman *et al* [8] suggest that as the power law exponent decreases, so the flow moves further away from Newtonian, and the transitional value of Re_w increases. Their experiments indicate that transition occurs for $Re_w \in [1300, 3000]$. However, in [2] it is stated that for drag-reducing polymers the transition point is located at approximately the same Reynolds number as for the (Newtonian) solvent $Re \approx 2300$. The experimental results of Slatter [13] confirm this by showing that choosing Re_3 anywhere in the range $[2100, 2400]$ provides accurate results for the transition. The principal objective of Slatters work [9, 10, 11, 12, 13] was to establish a simple, single criterion for transition such as exists for Newtonian pipe flow e.g. $Re = 2300$ [13]. In Section 4 we will show that $Re_3 \sim 2300$ provides good agreement with experimental data.

The Reynolds number depends on both the velocity and pipe diameter. For a given pipe diameter, to maintain turbulent flow, the mean fluid velocity must be kept above a critical value V_c. The main focus of this work is to find a simple relation between the critical mean velocity, V_c, and the pipe diameter, D, for large pipes. For sufficiently large pipes, $D = \mathcal{O}(1)\,\text{m}$, experimental observations indicate that the critical velocity becomes independent of the pipe diameter. In this limit, dimensional analysis shows that the dependence of V_c then takes the form

$$V_c = C(n)\sqrt{\frac{\tau_y}{\rho}}\ . \tag{5}$$

However, the dimensional analysis cannot determine the form of the coefficient $C(n)$, which must at present be approximated numerically for a given fluid. Our goal is therefore to find an analytical expression for $C(n)$.

The structure of the report is as follows. In Section 2 we reproduce s-tandard results to describe the flow of a Herschel-Bulkley fluid in a pipe. In Section 3 these results are used to determine the large and small diameter pipe asymptotes on the critical velocity-pipe diameter diagram. In particular we determine an analytical expression for $C(n)$. In Section 4 we compare our analytical model with the experimental data of Slatter [13].

2 Determination of the velocity profile in a pipe

Under conditions of fully developed, steady-state, one dimensional laminar pipe flow, a yield-stress fluid will shear in the annular region next to the pipe wall. Near the centre of the pipe, where the applied shear stresses are less than the yield stress, there will be a solid, unsheared plug which is carried along by the applied pressure gradient at the highest velocity. Velocity profiles are quoted in [3, 7] and a brief derivation is given in [4, 14] using a force balance. The plug region is discussed in [14] but with no details on how to determine the transition point between plug and fluid regions.

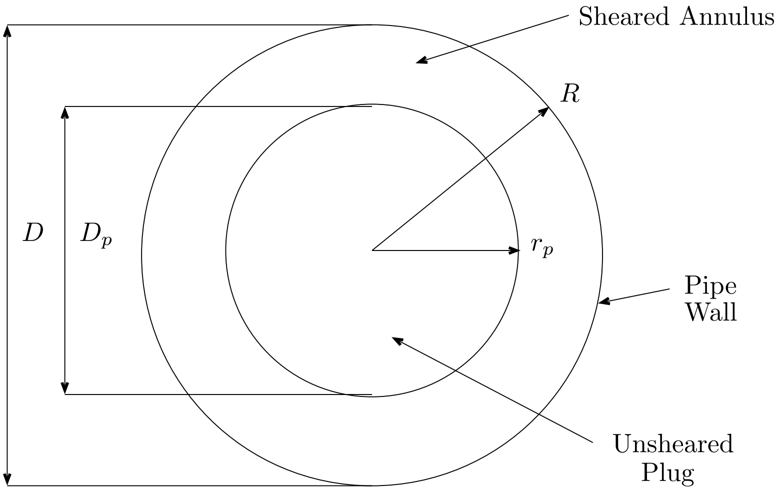

Figure 1: Steady, unidirectional flow geometry.

2.1 Governing equations

The flow geometry is depicted in Figure 1. A plug, with diameter $D_p = 2r_p$, is surrounded by an annulus of moving fluid through a pipe of diameter D. We assume that the flow is unidirectional and steady. Consequently we may write the velocity vector as $\mathbf{u} = (0, w(r))$. The z axis lies along the centreline of the pipe and w is the velocity in the z direction. The shear stress depends on w_r, and so is also independent of z. The Navier-Stokes equations therefore reduce to the simple form

$$\frac{\partial p}{\partial r} = 0 \ , \qquad \frac{1}{r}\frac{\partial}{\partial r}(r\tau) = \frac{\partial p}{\partial z} \ . \tag{6}$$

The first equation indicates $p = p(z)$ and so the second may be integrated to give

$$\tau = \frac{r}{2}\frac{dp}{dz} + \frac{c_0}{r} \ , \tag{7}$$

where c_0 is the integration constant. After the stress-strain relation has been specified, equation (7) must be solved subject to four boundary conditions: symmetry at $r = 0$, zero velocity at $r = R$ and continuity of velocity and stress at the yield surface $r = r_p$,

$$\left.\frac{dw}{dr}\right|_{r=0} = 0 \ , \qquad w(R) = 0 \ , \qquad [w]_{r=r_p} = [\tau]_{r=r_p} = 0 \ . \tag{8}$$

2.2 Biviscosity model

At this stage we must specify a shear stress relation. Perhaps the simplest way to mathematically deal with a yield stress fluid is to begin with a biviscosity model. Once the velocities are determined in the two regions we let the viscosity become infinite in the low stress region, thus producing a solid central region. Note, if the analysis is carried through from the start with a central plug then there is no way to determine the plug velocity. We therefore approximate the Herschel-Bulkley fluid model by

$$\tau = \begin{cases} \eta_1 \dfrac{dw}{dr} \ , & |\tau| < \tau_m \\ -\tau_c - K\left(-\dfrac{dw}{dr}\right)^n \ , & |\tau| > \tau_m \ , \end{cases}$$

where η_1 is the viscosity for low shears and K is the consistency index for high shear, τ_m is the shear stress where the two models coincide and $-\tau_c$ is the intercept of the second viscosity model with the τ axis. We have taken $-\tau_c$ since $w_r < 0$ throughout the pipe, and so the shear stress will be negative everywhere. In the limit $\eta_1 \to \infty$ both stresses tend to the yield stress, $\tau_c, \tau_m \to \tau_y$. The relation between stress and shear rate is shown in Figure 2.

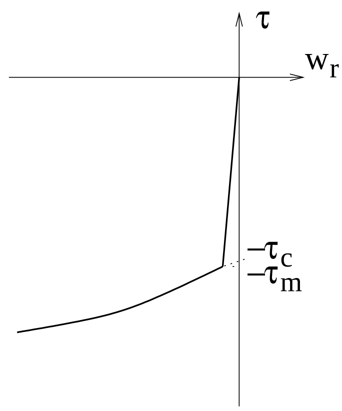

Figure 2: Stress versus shear rate for a biviscosity fluid.

In the central region of the pipe the shear stress is low and so we substitute the stress relation for $|\tau| < \tau_m$ into equation (7):

$$\eta_1 \frac{dw_1}{dr} = \frac{r}{2}\frac{dp}{dz} + \frac{c_0}{r} \ , \tag{9}$$

where, to avoid confusion we write $w = w_1$ in this region. At $r = 0$, the gradient is zero and so $c_0 = 0$. The fluid velocity in the 'plug' region is therefore given by

$$w_1 = \frac{r^2}{4\eta_1}\frac{dp}{dz} + c_1 \ , \qquad\qquad r \leq r_p \ . \tag{10}$$

The constant c_1 can only be determined once we have calculated w_2, the fluid velocity away from the plug.

The radius of the plug region may now be determined. At the yield surface the stress $|\tau| = \tau_m$ and so

$$-\tau_m = \eta_1 \frac{dw_1}{dr} = \frac{r_p}{2}\frac{dp}{dz} \tag{11}$$

which implies that

$$r_p = -\frac{2\tau_m}{p_z} \ . \tag{12}$$

Note that the plug radius depends only upon the yield stress and pressure gradient and is independent of the fictitious viscosity η_1. The same result may be obtained using the velocity profile in the annular flow region.

The region close to the pipe wall is subject to high shear and we substitute the expression for $|\tau| > \tau_m$ into (7):

$$-K\left(-\frac{dw_2}{dr}\right)^n = \tau_c + \frac{r}{2}\frac{dp}{dz} + \frac{c_2}{r} \ . \tag{13}$$

At present, we cannot integrate this equation but progress can be made by imposing continuity of shear stress at $r = r_p$:

$$\eta_1 \frac{dw_1}{dr} = -\tau_c - K\left(-\frac{dw_2}{dr}\right)^n \tag{14}$$

and therefore

$$\frac{r_p}{2}\frac{dp}{dz} = -\tau_c + \tau_c + \frac{r_p}{2}\frac{dp}{dz} + \frac{c_2}{r_p} \ . \tag{15}$$

This shows that $c_2 = 0$ and we can now integrate equation (13) subject to $w(R) = 0$ to give

$$w_2 = \frac{2n}{(n+1)p_z K^{1/n}}\left[\left(-\frac{p_z r}{2} - \tau_c\right)^{(n+1)/n} - \left(-\frac{p_z R}{2} - \tau_c\right)^{(n+1)/n}\right] \ . \tag{16}$$

The final unknown c_1, in equation (10), is determined by imposing continuity of velocity at $r = r_p$:

$$\frac{r_p^2}{4\eta_1}\frac{dp}{dz} + c_1 = \frac{2n}{(n+1)p_z K^{1/n}}\left[\left(-\frac{p_z r_p}{2} - \tau_c\right)^{(n+1)/n} - \left(-\frac{p_z R}{2} - \tau_c\right)^{(n+1)/n}\right] \ . \tag{17}$$

Using equation (12) the velocity in the plug region may now be written

$$w_1 = \frac{(r^2 - r_p^2)}{4\eta_1}\frac{dp}{dz} + \frac{2n}{(n+1)p_z K^{1/n}}\left[(\tau_m - \tau_c)^{(n+1)/n} - \left(-\frac{p_z R}{2} - \tau_c\right)^{(n+1)/n}\right] \ . \tag{18}$$

In the limit $\eta_1 \to \infty$ we find the true plug velocity

$$w_1 = -\frac{2n}{(n+1)p_z K^{1/n}} \left(-\frac{p_z R}{2} - \tau_y\right)^{(n+1)/n} . \tag{19}$$

The velocity profile in the pipe is now specified for a Herschel-Bulkley fluid by equations (16) and (19), where the first holds for $r_p \leq r \leq R$ and the second for $0 \leq r \leq r_p$. We can retrieve the result given in [9] by first calculating the wall shear stress and replacing the radius with the pipe diameter, $R = D/2$. In general the stress in the fluid region is

$$\tau = -\tau_y - K\left(-\frac{dw_2}{dr}\right)^n = \frac{p_z r}{2} , \tag{20}$$

where we have replaced τ_c with τ_y now that $\eta_1 \to \infty$. The wall shear stress, $\tau = -\tau_0$, is obtained by setting $r = R$. This also allows us to remove the pressure gradient $p_z = -4\tau_0/D$. Hence we may write the velocity in the fluid region as

$$w = \frac{Dn}{2(n+1)\tau_0 K^{1/n}} \left[(\tau_0 - \tau_y)^{(n+1)/n} - (\tau - \tau_y)^{(n+1)/n}\right] . \tag{21}$$

The plug velocity $w = w_1$ can be obtained by setting $\tau = \tau_y$ in (21)

$$w_p = \frac{Dn}{2(n+1)\tau_0 K^{1/n}} (\tau_0 - \tau_y)^{(n+1)/n} . \tag{22}$$

In Figure 3 two velocity profiles are shown for flow in a pipe with $p_z = -600$, $\tau_y = 10$, $D = 0.1$, $K = 0.005$ and two values for the power $n = 0.9, 1$. These values result in a plug radius $r_p = 0.0333$m (independent of n). The plug radius is marked with a $*$. The shear thinning fluid, with $n = 0.9$, moves faster than the Bingham fluid.

The mean fluid velocity in the pipe, V, is defined as

$$V = \frac{2\pi}{\pi R^2}\left[\int_0^{r_p} r w_p \, dr + \int_{r_p}^{R} r w \, dr\right] \tag{23}$$

$$= \frac{Dn}{2K^{1/n}\tau_0^3}(\tau_0 - \tau_y)^{(n+1)/n}\left[\frac{(\tau_0 - \tau_y)^2}{3n+1} + \frac{2\tau_y(\tau_0 - \tau_y)}{2n+1} + \frac{\tau_y^2}{n+1}\right] . \tag{24}$$

This will be used in Section 3 to determine the transitional velocity.

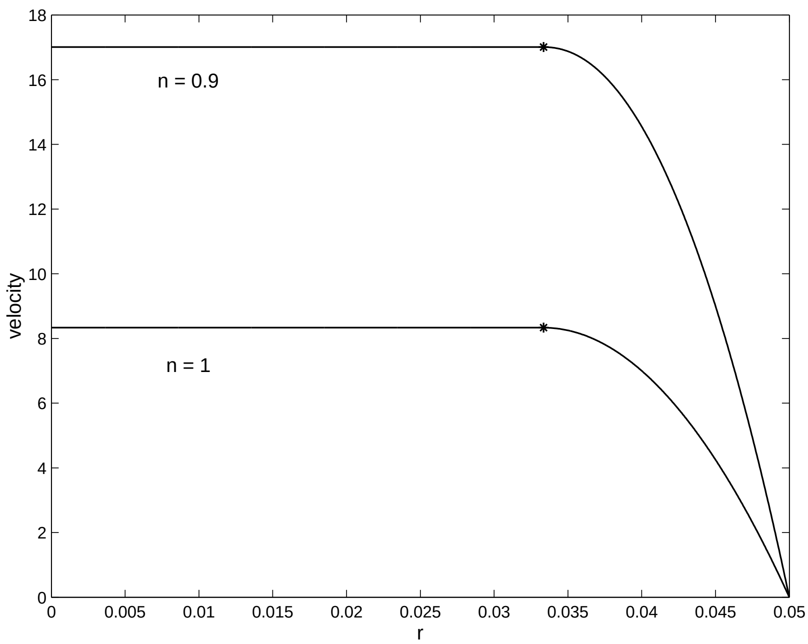

Figure 3: Velocity profiles for two Herschel-Bulkley fluids ($K = 0.005$, $p_z = -600$ and $\tau_y = 10$), with $n = 0.9$ and $n = 1$.

2.3 Force balance derivation

An alternative way to derive the velocity profile in a Herschel-Bulkley fluid is to use a force balance, see [4, 14] for example. A simple force balance on a cylindrical element of radius r and length $\mathrm{d}L$ yields

$$-\pi r^2 \mathrm{d}p = 2\pi r \tau \mathrm{d}L \qquad \text{which implies} \qquad \tau = -\frac{r}{2}\frac{\mathrm{d}p}{\mathrm{d}L} \ . \tag{25}$$

Then for the Herschel-Bulkley flow we know that τ satisfies

$$\tau = \tau_y + K\dot{\gamma}^n \ , \tag{26}$$

where $\dot{\gamma}$ is the modulus of the shear rate, which is simply $-w_r$ in a pipe. Combining (25) and (26) gives

$$-\frac{dw}{dr} = \frac{1}{K^{1/n}}\left(-\frac{r}{2}\frac{\mathrm{d}p}{\mathrm{d}L} - \tau_y\right)^{1/n} \ . \tag{27}$$

After integrating and applying the no-slip condition on $r = R$, we obtain

$$w = \frac{2n}{(n+1)} \frac{1}{K^{1/n}\left(-\frac{\mathrm{d}p}{\mathrm{d}L}\right)} \left[\left(-\frac{R}{2}\frac{\mathrm{d}p}{\mathrm{d}L} - \tau_y \right)^{(n+1)/n} - \left(-\frac{r}{2}\frac{\mathrm{d}p}{\mathrm{d}L} - \tau_y \right)^{(n+1)/n} \right] , \qquad (28)$$

which is obviously identical to w_2 in (16).

3 Asymptotes for large and small D

Now that the velocity profile has been calculated we can determine the relation between the Reynolds number Re_3, the mean velocity V and the pipe diameter D. The aim of this analysis is to find the critical velocity, $V = V_c$, above which the flow is turbulent. As discussed in the introduction this occurs when $Re_3 \sim 2300$. So the following analysis will lead to a relation of the form $V = f(Re_3, D)$ and by setting $Re_3 = 2300$ we determine the relation between V_c and D.

The definition for Re_3 is given by equation (4) where

$$V_a = \frac{Q_a}{A_a} , \qquad D_a = D - D_p = 2(R - r_p) , \qquad (29)$$

represent the average velocity and diameter of the annular region. The flux in the annular region is the total flux minus the flux of the plug region:

$$Q_a = Q - Q_p = Q - w_p A_p = Q - w_p \pi r_p^2 , \qquad (30)$$

and so

$$V_a = \frac{Q - w_p \pi r_p^2}{\pi(R^2 - r_p^2)} . \qquad (31)$$

Equations (12) and (22) define r_p and w_p respectively. The total flux $Q = VA = V\pi R^2$. From the definition of the stress (20) we find the ratio $r_p/R = \tau_y/\tau_0$. Using this and the definitions of V and w_p we may write V_a in (31) as

$$\begin{aligned} V_a = \frac{V\pi R^2 - w_p \pi r_p^2}{\pi(R^2 - r_p^2)} &= \frac{V\tau_0^2 - w_p \tau_y^2}{\tau_0^2 - \tau_y^2} \\ &= \frac{Dn}{2K^{1/n}} \frac{(\tau_0 - \tau_y)^{(n+1)/n}}{\tau_0(\tau_0 + \tau_y)} \left[\frac{\tau_0 - \tau_y}{3n+1} + \frac{2\tau_y}{2n+1} \right] . \qquad (32) \end{aligned}$$

Similarly D_a from (29) becomes

$$D_a = \frac{D(\tau_0 - \tau_y)}{\tau_0} \ . \tag{33}$$

We now proceed to determine the large and small D asymptotes. The large D asymptote is the most physically interesting; industrial slurries are seldom transported through narrow pipes. However, we will start with the small D case since this is the simplest to deal with analytically.

3.1 The small D asymptote

As $D \to 0$ then the high shear rates required to move the fluid will confine the plug to a small region near $r = 0$. This means that $r_p \ll R$ and consequently $D_a \approx D$ and the average annular velocity $V_a \approx V$. Furthermore, since $r_p/R = \tau_y/\tau_0 \ll 1$ the wall stress is much greater than the yield stress. In the limit $\tau_y \ll \tau_0$ the average velocity defined by (24) (or equation (32) since $V_a \approx V$) becomes

$$V_a = V = \frac{Dn\tau_0^{1/n}}{2K^{1/n}(3n+1)} \ , \tag{34}$$

to leading order in τ_y/τ_0. The relation (34) shows that the term involving τ_y in the denominator of Re_3 defined by (4) may be neglected since

$$\tau_y + K\left(\frac{8V_a}{D_a}\right)^n = \tau_y + \tau_0\left(\frac{4n}{3n+1}\right)^n \approx \tau_0\left(\frac{4n}{3n+1}\right)^n \ ,$$

provided $n \gg (\tau_y/\tau_0)^{1/n}/4$. Hence the Reynolds number may be written

$$Re_3 \approx \frac{8\rho V^2}{K}\left(\frac{D}{8V}\right)^n \ .$$

Rearranging this gives an expression for V in terms of D

$$V = \left(\frac{8^{n-1}KRe_3}{\rho D^n}\right)^{1/(2-n)} \ , \tag{35}$$

which defines the small D asymptote. The critical velocity V_c is then obtained by setting the Reynolds number to the critical value $Re_3 = 2300$. Note that $V \sim D^{-n/(2-n)}$ and in the Bingham limit $n = 1$, then $V \sim 1/D$ for small D.

3.2 The large D asymptote

Given that τ_y, K and n are fluid properties, then by inspection of equation (24) we can see that for a fixed value of V, as the pipe diameter D is increased, the wall stress value must approach the yield stress [9], $\tau_0 \to \tau_y$ as $D \to \infty$. Thus for large D a high proportion of the slurry will be at the yield stress and the plug therefore occupies most of the pipe. Experiments also show that the transition velocity V_c becomes independent of D as $D \to \infty$ [9]. From examining (24) it is clear that the only way the velocity can become independent of D is if $(\tau_0 - \tau_y)^{(n+1)/n} = \mathcal{O}[D^{-1}]$ as $D \to \infty$. This motivates us to look for an expansion of $\tau_0 - \tau_y$ in terms of the small parameter $\epsilon = D^{-n/(n+1)}$,

$$\begin{aligned} \tau_0 &= \tau_y + \alpha_0 D^{-n/(n+1)} + \alpha_1 D^{-2n/(n+1)} + \mathcal{O}((D^{-n/(n+1)})^3) \\ &= \tau_y + \epsilon\alpha_0 + \epsilon^2\alpha_1 + \mathcal{O}(\epsilon^3) \ , \end{aligned} \tag{36}$$

where the expansion is valid provided $\epsilon \ll \tau_y/\alpha_0$, $\epsilon\alpha_1 \ll \alpha_0$. The constants $\alpha_i = \mathcal{O}(1)$ are unknown at present and are determined as part of the analysis below.

Before substituting V_a and D_a into (4), it is convenient to replace τ_0 using (36) to find the dominant terms from these expressions. Thus, neglecting terms of $\mathcal{O}(\epsilon^3)$,

$$\begin{aligned} V_a &= \frac{Dn}{2K^{1/n}} \frac{(\epsilon\alpha_0)^{(n+1)/n}\,(1+\epsilon\alpha_1/\alpha_0)^{(n+1)/n}}{\tau_y^2\,(1+\epsilon\alpha_0/\tau_y+\epsilon^2\alpha_1/\tau_y)\,(2+\epsilon\alpha_0/\tau_y+\epsilon^2\alpha_1/\tau_y)} \\ & \left[\frac{2\tau_y}{2n+1} + \frac{\epsilon\alpha_0(1+\epsilon\alpha_1/\alpha_0)}{3n+1}\right] \ . \end{aligned}$$

To first order in ϵ this reduces to

$$V_a = \frac{n\alpha_0^{(n+1)/n}}{2(2n+1)K^{1/n}\tau_y}\left[1 + \left\{\frac{(n+1)\alpha_1}{n\alpha_0} - \frac{(7n+2)\alpha_0}{2(3n+1)\tau_y}\right\}\epsilon\right] \tag{37}$$

and similarly

$$D_a = D\left(\frac{\tau_0-\tau_y}{\tau_0}\right) = \frac{\epsilon D\alpha_0}{\tau_y}\left[1 + \left(\frac{\alpha_1}{\alpha_0} - \frac{\alpha_0}{\tau_y}\right)\epsilon\right] \ . \tag{38}$$

Note that since D is large, the term $\epsilon D = D^{1/(n+1)} \gg \epsilon$. Using these expressions we find

$$\frac{8V_a}{D_a} = \frac{4n\alpha_0^{1/n}\epsilon^{1/n}}{(2n+1)K^{1/n}}\left[1 + \left(\frac{\alpha_1}{n\alpha_0} - \frac{n\alpha_0}{2\tau_y(3n+1)}\right)\epsilon\right] \ .$$

To first order in ϵ the Reynolds number Re_3 becomes

$$Re_3 = \frac{2\rho n^2 \alpha_0^{2(n+1)/n}}{(2n+1)^2 K^{2/n} \tau_y^3} \left[1 + \left\{ \frac{2(n+1)\alpha_1}{n\alpha_0} - \frac{\alpha_0}{\tau_y} \left(\left(\frac{4n}{2n+1} \right)^n + \frac{7n+2}{3n+1} \right) \right\} \epsilon \right] . \tag{39}$$

This expression permits us to determine α_0, α_1. The leading order terms on the right hand side balance with Re_3, the first order terms must be zero. Therefore

$$\alpha_0 = \left(\frac{(2n+1)^2 K^{2/n} \tau_y^3 Re_3}{2\rho n^2} \right)^{n/(2(n+1))} ,$$

$$\alpha_1 = \frac{n\alpha_0^2}{2\tau_y(n+1)} \left(\left(\frac{4n}{2n+1} \right)^n + \frac{7n+2}{3n+1} \right) . \tag{40}$$

Equation (39) provides a relation between Re_3 and D (through the small parameter ϵ). We must now bring in the mean velocity to find the relation between V and D.

The mean velocity, defined by (24), to first order in ϵ is

$$V = \frac{n\alpha_0^{(n+1)/n}}{2(n+1)K^{1/n}\tau_y} \left[1 + \left(\frac{n+1}{n} \frac{\alpha_1}{\alpha_0} - \frac{4n+1}{2n+1} \frac{\alpha_0}{\tau_y} \right) \epsilon \right] . \tag{41}$$

Writing $V = V_0 + \epsilon V_1$ we can identify the leading and first order terms

$$V_0 = \frac{n\alpha_0^{(n+1)/n}}{2(n+1)K^{1/n}\tau_y} , \qquad V_1 = V_0 \left(\frac{n+1}{n} \frac{\alpha_1}{\alpha_0} - \frac{4n+1}{2n+1} \frac{\alpha_0}{\tau_y} \right) . \tag{42}$$

Substituting for α_0, via equation (40), in the expression for V_0 and rearranging leads to

$$V_0 = \frac{2n+1}{n+1} \sqrt{\frac{Re_3}{8}} \sqrt{\frac{\tau_y}{\rho}} = C(n) \sqrt{\frac{\tau_y}{\rho}} . \tag{43}$$

As discussed in the introduction, finding the expression in (43) is our main goal. This equation identifies the asymptote as $D \to \infty$ and the form of the fluid constant $C(n)$. However, using the correction term V_1 we can find the form of the curve for smaller D and so get closer to the transition between the small and large D asymptotes.

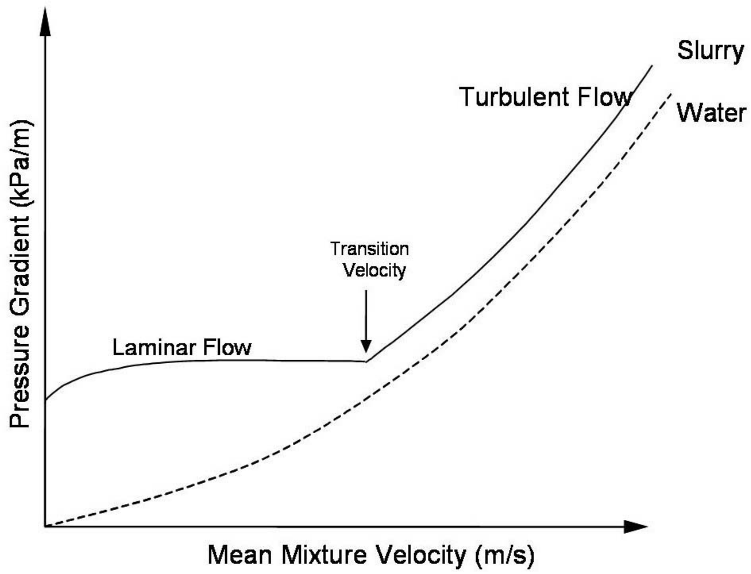

Figure 4: Schematic of velocity against pressure gradient for water and slurry flows.

4 Results

The material under test is pumped through a pipe test rig over a range of velocities [9, 13]. The data is then compared with the expression for average velocity, equation (26). In laminar flow, the data agrees closely, whereas, in turbulent flow, the data departs sharply. Transition is identified as that point at which the data begins to depart from equation (26). Figure 4 depicts this transition. With a Newtonian fluid the velocity increases monotonically with the pressure gradient. With a slurry, initially the stress must overcome the yield stress before flow starts. The velocity then increases rapidly with a small change in pressure gradient until a sharp transition is reached, beyond which a much greater change in pressure is required to increase the mean velocity. The point where this transition occurs defines our critical velocity and this is how the data points in Figure 6 are calculated.

The goal of this analysis is to find the critical velocity, V_c, which determines

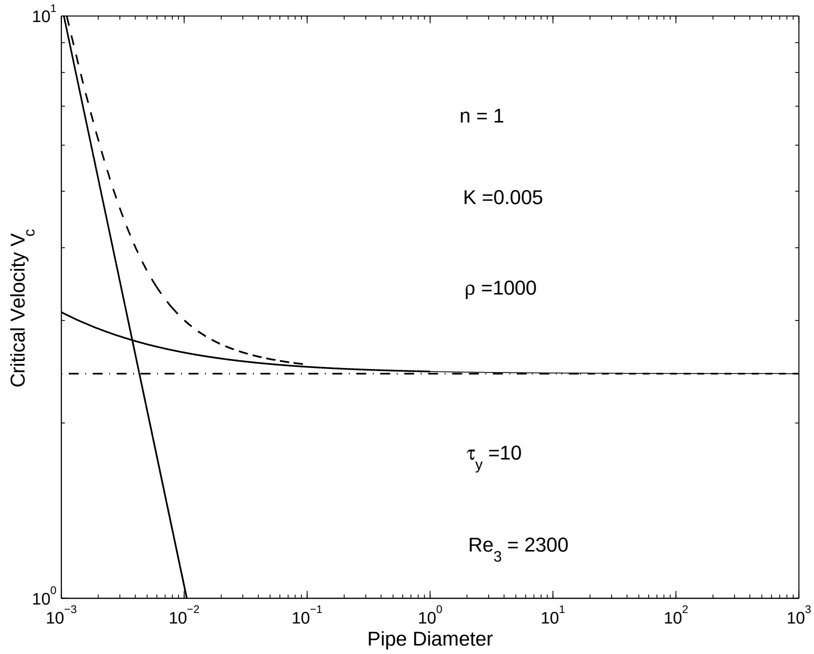

Figure 5: Plot of critical velocity against pipe diameter for a Bingham fluid. The dashed line denotes the exact solution, the solid lines denote the small (left) and large (right) D asymptotes and the dot-dashed line denotes the leading order large D asymptote.

the transition to turbulent flow. In our numerical calculations we varied the value of Re_3 to obtain the best fit with experimental data. Excellent results were obtained by setting $Re_3 = 2300$ and these are presented in the figures.

In Figure 5 we plot the critical velocity V_c against D for a Bingham fluid. The dotted line is the asymptote defined by setting $Re_3 = 2300$ in equation (43). This gives $V_c = 2.43$. The correction to the leading order result $V = V_0 + \epsilon V_1$ is shown as the solid line that matches the horizontal asymptote for large D (i.e. D approximately greater than 1m). The two lines noticeably diverge for $D < 6$m. The dashed line represents the exact solution calculated numerically from equations (4) and (32). On the left is another solid line representing the small D asymptote of equation (35). For large D it is clear that the asymptotic and exact results show excellent agreement. As D decreases, $D < 1$m, the results move away from the leading order value for critical velocity.

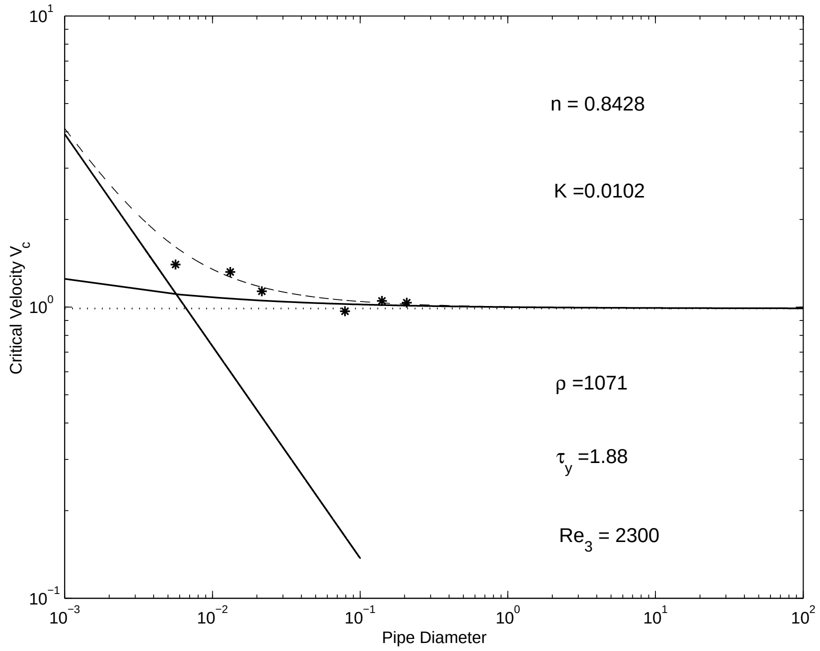

Figure 6: Plot of critical velocity against pipe diameter for a Herschel-Bulkley fluid. The $*$'s denote the experimental data, the dashed line denotes the exact solution, the solid lines denote the small (left) and large (right) D asymptotes.

The first order correction permits the asymptotic solution to be comparable with the exact solution down to $D \approx 0.1$m. Below this value the critical velocity increases rapidly. For $D < 2$mm the small D asymptote provides a good approximation to the exact solution.

In Figure 6 we show results for a Herschel-Bulkley fluid with $n = 0.8428$. The experimental data points, marked with a '*', are taken from [9]. The results show the same behaviour as in Figure 5. For large D the leading order and first order correction tend to the same value, in this case $V_c \approx 0.989$. They noticeably diverge for $D < 0.1$m. In the case $D \approx 1$mm the small D asymptote provides a good approximation. In addition, good agreement with the experimental results can be observed.

5 Conclusion

The main aim of the work described in this paper has been to determine an analytical form for the coefficient $C(n)$ in the expression for the critical velocity at large pipe diameters. To achieve this we first had to calculate the velocity profile in a pipe for a Herschel-Bulkley fluid. It was discovered that for large D the wall stress was close to the yield stress. This allowed us to simplify the solutions using an asymptotic expansion based on the difference $\tau_0 - \tau_y \ll 1$. At leading order we could then determine an expression for $C(n) = (2n+1)\sqrt{Re_3}/((n+1)\sqrt{8})$.

The work shows that by using Re_3 as the non-dimensional grouping to describe the transition to turbulence leads to the correct behaviour at large and small pipe diameters. In particular it was found that the transition occurs around $Re_3 = 2300$ for a yield stress fluid, for both large and small diameters.

Comparison with experimental data for a Herschel-Bulkley fluid shows that both large and small D asymptotes are accurate for a large range of pipe diameter, provided we set $Re_3 = 2300$. In general we found the intermediate region, where neither approximation holds, is typically between 1mm and 1cm, which is of little practical interest.

In future it is intended to extend both small and large D asymptotics, with the hope of better matching in the intermediate region. Further comparison with experimental data will be carried out including an investigation into the critical value of Re_3, for both large and small diameters.

6 Nomenclature

τ	shear stress	w	velocity
p	pressure	V	mean fluid velocity
R	pipe radius	D	pipe diameter
η	fluid viscosity	ρ	density
τ_y	yield stress	τ_0	wall shear stress
K	fluid consistency index	n	flow behaviour index
Re	Reynolds number	Q	flux
V_c	critical velocity	$\dot{\gamma}$	modulus of shear rate

subscript a denotes annulus   subscript p denotes plug

References

[1] Chhabra, R.P. and Richardson, J.F. Non-Newtonian flow in the process industries, Butterworth-Heinemann (1999).

[2] Draad, A.A., Kuiken, G.D.C. and Nieuwstadt, F.T.M. Laminar-turbulent transition in pipe flow for Newtonian and non-Newtonian fluids. *J. Fluid Mech.,* **377**(1998), 267–312.

[3] Escudier, M.P. and Presti, F. Pipe flow of a thixotropic liquid. *J. Non-Newtonian Fluid Mech.* **62** (1996), 291–306.

[4] Govier, G.W. and Aziz, K. The Flow of Complex Mixtures in Pipes. *Litton Educational Pub. Inc.* (1972).

[5] Honey, H.C. and Pretorius, W.A. Laminar flow pipe hydraulics of pseudoplastic-thixotropic sewage sludges. Water SA 26(1) (2000), 19–25.

[6] Metzner, A.B. and Reed, J.C. Flow of non-Newtonian fluids - correlation of the laminar, transition and turbulent flow regions. *AIChE J.* **1** (1955), 434–440.

[7] Peixinho, J., Nouar, C., Desaubry, C. and Théron B. Laminar transitional and turbulent flow of yield stress fluid in a pipe. *J. Non-Newtonian Fluid Mech.,* **128** (2005), 172–184.

[8] Rudman, M., Blackburn, H.M., Graham, L.J.W. and Pullum, L. Turbulent pipe flow of shear thinning fluids. *J. Non-Newtonian Fluid Mech.,* **118** (2004), 33–48.

[9] Slatter, P.T. The role of the yield stress on the laminar/turbulent transition. Ninth Int. Conf. on Transport and Sedimentation of Solid Particles, Cracow, Poland, (1997), pp 547–561.

[10] Slatter, P.T. and Wasp, E.J. The laminar/turbulent transition in large pipes. 10th Int. Conf. on Transport and Sedimentation of Solid Particles, Wroclaw: 4-7 September, 2000, pp 389–399.

[11] Slatter, P.T. and Lazarus, J.H. Critical flow in slurry pipelines. 12th Int. Conf. on slurry handling and pipeline transport, Hydrotransport 12 BHR Group, (1993), p 639.

[12] Slatter, P.T. The role of rheology in the pipelining of mineral slurries. *Min. Pro. Ext. Met. Rev.*, **120** (1999), 281–300.

[13] Slatter, P.T. The laminar/turbulent transition prediction for non- Newtonian slurries. Proc. Int. Conf. Problems in Fluid Mechanics and Hydrology, Academy of Sciences of the Czech Republic, Prague, 23-26 June, 1999, pp 247–256.

[14] Soto, R.J. and Shah, V.L. Entrance flow of a yield-power law fluid. *Appl. Sci. Res.* **32** (1976), 73–85.

[15] Pinho, F.T. and Whitelaw, J.H. Flow of non-Newtonian fluids in a pipe. *J. Non-Newtonian Fluid Mech.,* **34** (1990), 129–144.

[16] Wasp, E.J., Kenny, J.P. and Gandhi, R.L. Solid-liquid flow: slurry pipeline transportation, Trans Tech Publications, New York (1977).